Nigerian Journal of Physics (NJP)
ISSN online: 3027-0936
ISSN print: 1595-0611
DOI: https://doi.org/10.62292/njp.v33i4.2024.334
Volume 33(4), December 2024

Synthesis and Characterization of Nickel-Doped Cerium Oxide Thin Films Using Solution Growth Technique

***[1]Mbamara, C., [2,3]Nworie, I. C. [2,3]Brown, N. W., [2,3]Otah, P. B., [4]Oko, K. I., [2,5]Idu, H. K. and [6]Amadi, M. C.**

[1]Department of Industrial Physics, University of Agriculture and Environmental Science, Umuagwo, Imo State, Nigeria
[2]Department of Industrial and Medical Physics, David Umahi Federal University of Health Sciences (DUFUHS), Uburu Ebonyi State, Nigeria
[3]International Institute for Machine Learning, Robotics & Artificial Intelligence Research, (DUFUHS) Ebonyi State, Nigeria
[4]Department of Science Education, Ebonyi State University, Abakaliki
[5]International Institute for Nuclear Medicine & Allied Health Research, (DUFUHS) Ebonyi State, Nigeria
[6]Department of Biochemistry, University of Agriculture and Environmental Science, Umuagwo, Imo State, Nigeria

[*]Corresponding author's email: bookfashion9@gmail.com Phone: +2347033038430

ABSTRACT

Metal-doped rare-earth oxides thin films, synthesized via solution growth, enable tunable electronic, optical, and catalytic properties for diverse technological applications due to their controlled composition and morphology. This study investigates the synthesis and characterization of Cerium Oxide (CeO_2) thin films doped with Nickel Oxide (NiO) using the Chemical Bath Deposition (CBD) technique. Reaction baths were prepared from solutions containing Cerium Nitrate, Nickel Sulphate, Sodium Hydroxide, Ammonia, and distilled water. The process involved the preparation of six reaction baths—three using Sodium Hydroxide and three using Ammonia as complexing agents, with varying concentrations of Cerium Nitrate. The deposited films were characterized for their optical and morphological properties. Optical measurements were conducted using a UV-spectrophotometer, revealing that Sodium Hydroxide resulted in lower transmittance and band gap energy compared to Ammonia at concentrations, indicating potential defects or impurities in the cerium oxide matrix. An increase in molar concentration corresponded with an elevated band gap energy, while the incorporation of NiO as a dopant significantly enhanced the band gap of the CeO_2 films. Morphological analysis via Scanning Electron Microscopy (SEM) demonstrated improved uniformity and orientation of the films with well-defined grain boundaries and reduced agglomeration when complexing agents were employed. These findings suggest that NiO-doped CeO_2 thin films exhibit promising potential for applications in photovoltaic systems, thermal control coatings, and UV radiation suppression.

Keywords:
Nickel Oxide,
Dopant,
Chemical bath Deposition,
Band gap,
Cerium Oxide.

INTRODUCTION

The increasing global demand for sustainable and renewable energy sources has driven significant research into materials that can improve energy efficiency and support alternative energy systems. One promising area of study is the development of thin film materials with enhanced optical and electronic properties. Among these materials, rare-earth oxides such as Cerium Oxide (CeO_2) have gained attention for their unique characteristics, including high thermal stability, excellent optical transparency, and catalytic activity (Bellardita *et al*, 2020; Melchionna *et al*, 2020). When doped with transition metals like Nickel Oxide (NiO), the properties of Cerium Oxide thin films can be further enhanced, making them suitable for a variety of advanced applications. Thin films are critical in many technological sectors, including solar energy conversion, optoelectronics, and thermal control coatings. The ability to tailor the properties of these films through doping and deposition techniques has

opened up new avenues for improving the performance of devices like solar cells, energy-efficient windows, and sensors (Baisnab *et al,* 2021; Dalapati *et al,* 2021). In particular, Nickel doping has the potential to modify the electronic structure and optical properties of Cerium Oxide, making it more versatile for practical applications (Mary *et al,* 2014). The properties of thin films depend heavily on the deposition method and growth parameters. There are various methods for thin film preparation, ranging from highly sophisticated techniques to simpler, cost-effective approaches. These methods can be broadly categorized into physical vapor deposition, chemical deposition, and liquid deposition techniques (Nworie *et al,* 2024).

In this study, the solution growth technique, specifically chemical bath deposition, which offers a cost-effective and scalable method for producing high-quality thin films (Nworie *et al,* 2024), was employed. This technique is known for its simplicity, affordability, and ability to control film thickness and uniformity by adjusting the concentration of chemical precursors and growth conditions. In order to achieve a controlled growth (Senguta *et al,* 2021) of the Nickel-doped Cerium Oxide films on glass substrates, Sodium Hydroxide and Ammonia were used as complexing agents during the deposition process. The films were examined through UV-VIS-NIR spectroscopy and Scanning Electron Microscopy (SEM) characterization to determine the effects of Nickel doping on the optical and morphological properties of the films. The analyzed properties were used in determining the potential applications of the films. Our aim is to gain a deeper understanding of how nickel doping modifies the properties of cerium oxide thin films. This knowledge can be applied in the development of advanced materials with improved performance in various technological applications.

MATERIALS AND METHODS

In this study, Cerium Oxide (CeO_2) thin films were doped with Nickel Oxide (NiO) using the Chemical Bath Deposition (CBD) technique. During the deposition process, reaction baths were prepared from solutions consisting of Cerium Nitrate, Nickel Sulphate, Sodium Hydroxide, Ammonia, and Distilled Water. At first, 0.1 M of Cerium Nitrate was measured into a 50 ml beaker and 100 ml of distilled water was added. This solution was stirred for 15 minutes using a magnetic stirrer, resulting in the formation of a light yellow solution. Similarly, 0.1 M of Nickel Sulphate was dissolved in 100 ml of distilled water in a separate beaker and stirred for 15 minutes. Subsequently, 15 ml of the Cerium Oxide solution was transferred to a 100 ml beaker, followed by the addition of 10 ml of Nickel Sulphate and 2 ml of Sodium Hydroxide. In another setup, 0.25 M of Cerium Oxide was combined with 10 ml of Nickel Sulphate and 2 ml of Ammonia in a separate beaker. This procedure was repeated to prepare a total of six reaction baths—three utilizing Sodium Hydroxide (NaOH) and three utilizing Ammonia as complexing agents. The solutions were mixed thoroughly to ensure homogeneity and transferred into separate beakers for deposition. Soda-lime glass substrates were meticulously cleaned with sulfuric acid and rinsed with distilled water. The cleaned substrates were then vertically immersed into the prepared solutions using synthetic foam holders. The deposition process was conducted over a period of three hours for each bath. Following deposition, the substrates were removed, rinsed with distilled water, and air-dried using clips. The optical properties of the thin films were characterized using a UV-spectrophotometer at the Centre for Energy Research and Development (CERD), Obafemi Awolowo University. This analysis involved measuring the interaction of electromagnetic radiation with the films to assess their transmittance and absorbance. Furthermore, the surface morphology and composition of the deposited films were examined using Scanning Electron Microscopy (SEM). SEM provided high-resolution images and detailed insights into the films' surface structure and elemental composition through the interaction of an electron beam with the sample surface. Utilizing the %T (percent transmission) data, all additional optical parameters were subsequently computed.

Theory: Transmittance (T)

Transmittance (T) is defined as the ratio of the radiant power (I) transmitted by a material to the total radiant power (I_0) incident on that material:

$$T = {}^{I}/_{I_o} \qquad (1)$$

In this context, I is referred to as the transmitted flux, while I_0 is the incident flux. When radiation from a source strikes a specimen, some of the radiation is absorbed, and some is scattered. For accurate transmission measurements, corrections must be made for reflection and scattering. The corrected transmittance is termed internal transmittance.

Transmittance can be categorized as either diffuse or specular. It is considered specular if only the emergent radiation parallel to the incident beam is measured; conversely, it is classified as diffuse if all emergent radiation is observed.

Given the thickness of a thin film (t), the absorption coefficient (α), and the reflectance (R), the radiation reaching the first interface is $(1-R)\ I_o$. The radiation reaching the second interface is $(1-R)\ I0\exp(-\alpha t)$, and only a fraction $(1-R)\ (1-R)\ I_0\exp(-\alpha t)$ emerges. The portion that is internally reflected eventually re-emerges, albeit with considerable attenuation. The final

expression, as described by Pankove (1971), can be represented as:

$$T = \frac{(1-R)^2 \exp(-at)}{(1-R)^2 \exp(-2at)} \quad (2)$$

In this equation, if the product αt is large, the term in the denominator can be neglected, and leading to the simplified expression for transmittance:

$$T = (1-R)^2 e^{-at} \quad (3)$$

Where R and t are known, transmittance can be calculated from the above equations. However, if R is unknown, the transmittance of two samples with different thicknesses, $t_1$and t_2, can be measured. The absorption coefficient α can then be determined from:

$$T_1/T_2 = e^{[a(t_2-t_1)]} \quad (4)$$

Band Gap (E_g)

The band gap (E_g) is defined as the energy required for an electron to transition from the upper part of the valence band to the conduction band. This energy gap typically ranges from 1 eV to 5 eV, depending on the material's conductivity. The band gap, also known as the energy gap, is largest in insulators, smaller in semiconductors, and negligible in good conductors. Thus, the nature of the energy bands indicates whether a material behaves as an electrical conductor or an insulator.

Thin films generally exhibit smaller band gaps compared to their bulk counterparts, which allows for greater carrier generation and higher photocurrent, especially in photovoltaic cells (Powalla *et al.*, 2018). In solar energy devices, such as solar cells, when photon or light radiation strikes the material, energy is released (Christian *et al.*, 2023). Even if the band gap of the window material is higher, the violet and ultraviolet parts of the solar spectrum can still penetrate the junction layer, generating more electron-hole pairs in the depletion region. The electron transitions from the upper part of the valence band to the lower part of the conduction band contribute to the shape of the absorption spectrum and the dispersion observed near the fundamental absorption edge (Nworie *et al.*, 2024).

The band gap is a critical parameter in material characterization, and detailed discussions on the absorption edge and band gaps can be found in the work of Jing *et al.* (2010). The band gap is expressed as:

$$Eg = hv - a^2 \quad (5)$$

Where: h = Planck's constant, v= frequency, and α = absorption coefficient.

Two types of attenuation occur when light rays or electromagnetic radiation penetrate a material. Some of this radiation undergoes scattering and reflection in all directions, while others are transformed into various forms of energy. The reflected radiation typically retains its energy, whereas absorbed radiation may exist as secondary radiation or be re-emitted.

The relationship between the absorption coefficient (α) and the incident photon energy (hv) is given by:

$$(\alpha hv)^n = A(hv - E_g) \quad (6)$$

Where A is a constant, (Eg) is the band gap of the material, and the exponent (n) depends on the type of electronic transition.

RESULTS AND DISCUSSION

Optical Characterization

Figures 1-4 present the transmittance spectra and band gap values for the thin films deposited at 0.1 M and 0.25 M concentrations of Cerium Oxide, respectively. These figures illustrate the optical behavior of the films, highlighting how concentration variations influence their transmittance and energy band gaps.

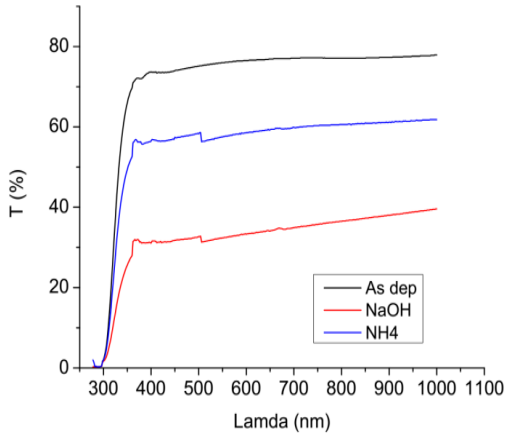

Figure 1: Transmittance vs lamda at 0.1M

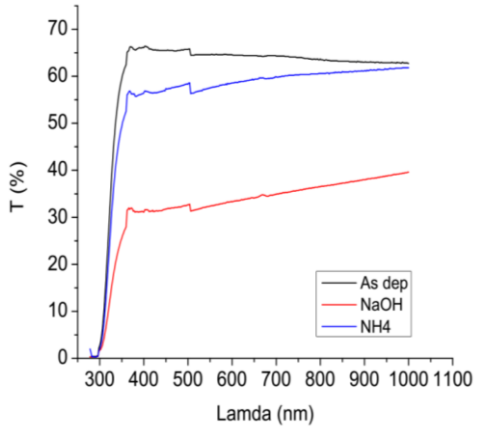

Figure 2: Transmittance vs lamda at 0.25M

Figures 1 and 2 displays the transmittance (T) versus wavelength (λ) plots for films deposited at a 0.1 M and 0.25 M concentrations respectively. The wavelength range analyzed was 240 nm to 1000 nm. The results indicate that the as-deposited films exhibited high transmittance in the visible region, typically greater than

70%. However, the introduction of complexing agents significantly affected the transmittance properties. As shown in Figure 1, films using ammonia as the complexing agent demonstrated transmittance levels below 60%, while those using NaOH exhibited the lowest transmittance, under 40%. These variations in transmittance can be attributed to the incorporation of complexing agent atoms, which act as dopants or impurities within the cerium oxide matrix. This doping effect leads to a reduction in transmittance. These findings align with the studies conducted by Göbel *et al.* (2010) and Tsud *et al.* (2010). In figure 2, Similar to the 0.1 M results, the as-deposited films exhibited high transmittance in the visible region, typically above 65%. The presence of complexing agents again had a significant effect. Ammonia-based films showed transmittance below 55%, while NaOH-based films had the lowest transmittance, fewer than 30%. The reduction in transmittance is similarly attributed to the introduction of complexing agent atoms acting as dopants or impurities in the cerium oxide structure. These results are consistent with the findings of Ershov *et al.* (2013).

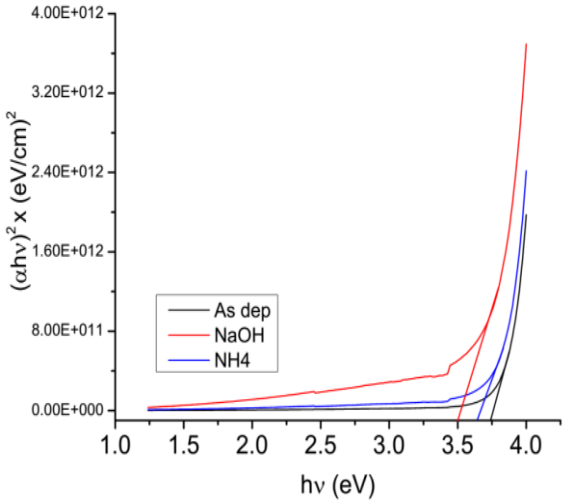

Figure 3: Plots of $(\alpha h\nu)^2$ vs $(h\nu)$ at 0.1M

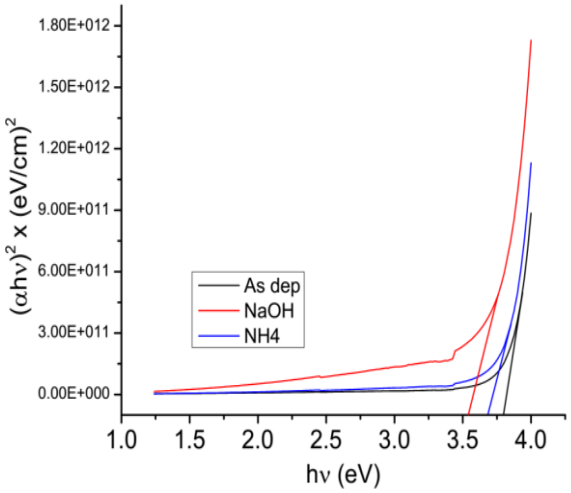

Figure 4: Plots of $(\alpha h\nu)^2$ vs $(h\nu)$ at 0.25M

Figures 3 and 4 presents the band gap for the films deposited at a concentration of 0.1 M and 0.25M respectively, with the energy band gap calculated using equation (6). A thorough analysis of the transmittance data indicates that the electronic transitions are of a direct nature. Consequently, a plot of $(\alpha h\nu)^2$ against photon energy was constructed to determine the optical band gap, which was obtained by extrapolating the linear segment near the absorption edge to the energy axis. The as-deposited film exhibited a band gap of 3.75 eV, while films utilizing sodium hydroxide and ammonia as complexing agents displayed band gaps of 3.5 eV and 3.63 eV, respectively. In Figure 4, analysis of the transmittance data revealed that the transitions were extensive. The as-deposited film exhibited a band gap of 3.76 eV, while films with sodium hydroxide and ammonia showed band gaps of 3.51 eV and 3.74 eV, respectively. These results indicate that the use of complexing agents decreased the band gap, bringing it closer to the optimal range for photovoltaic conversion and solar control coatings, consistent with the findings of Babitha *et al.* (2015).

Morphological Characterization

The morphological characterization results, obtained through Scanning Electron Microscopy (SEM), are presented in Figures 5-10. These figures provide detailed images of the surface structure and texture of the thin films, providing insights into how varying deposition conditions influence the morphology of the films. Figure 5 shows the morphological structure of the as-deposited film at a 0.1 M concentration. The analysis indicates a smooth surface with no visible irregularities. The film demonstrates strong interactions between the NiO nanostructures at the interface, which enhance the nanostructure morphology and promote good uniformity, as supported by Channei *et al.* (2013).

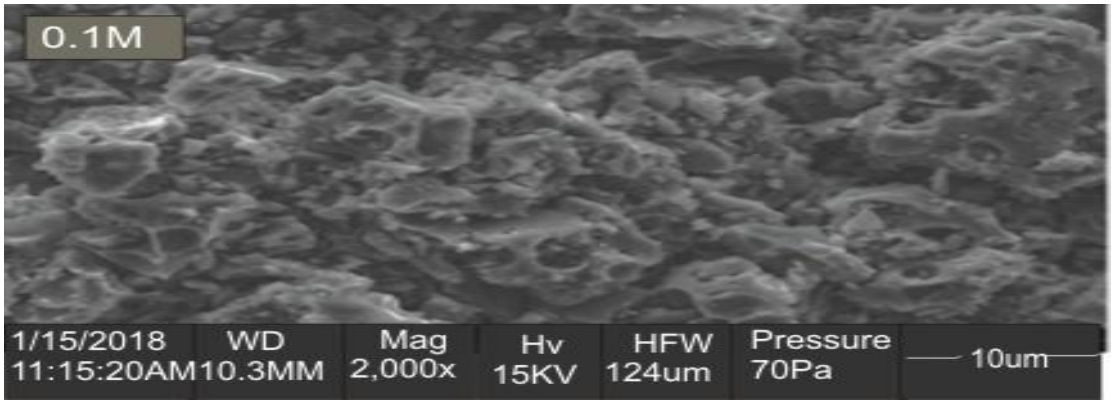

Figure 5: SEM Micrograph as-grown layer at 0.1 M

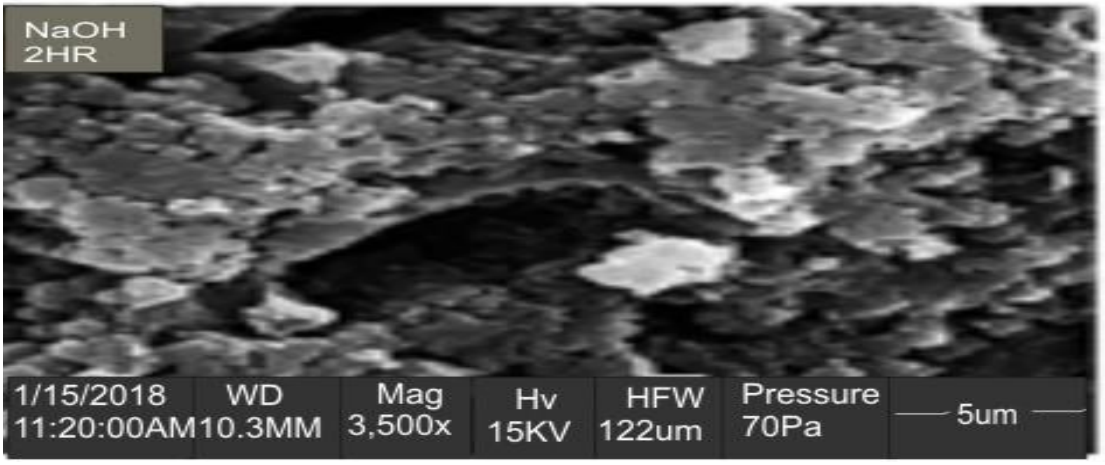

Figure 6: SEM Micrograph of the layer (0.1M) with NaOH as complexing agent

Figure 6 presents the SEM micrograph of the film with NaOH as the complexing agent. The image reveals that the addition of NaOH significantly improved the morphology of the film, resulting in reduced agglomeration and increased uniformity, consistent with the findings of Jaroslava *et al.* (2015).

Figure 7 shows the SEM micrograph of the film with ammonia as the complexing agent. The micrograph demonstrates that ammonia also enhanced the film's morphology. Notably, well-defined grain boundaries were observed, and the grains were homogeneous in shape and size, tightly packed with no visible pores. This was a marked improvement over the NaOH-complexed film, as noted by Adele et al. (2003).

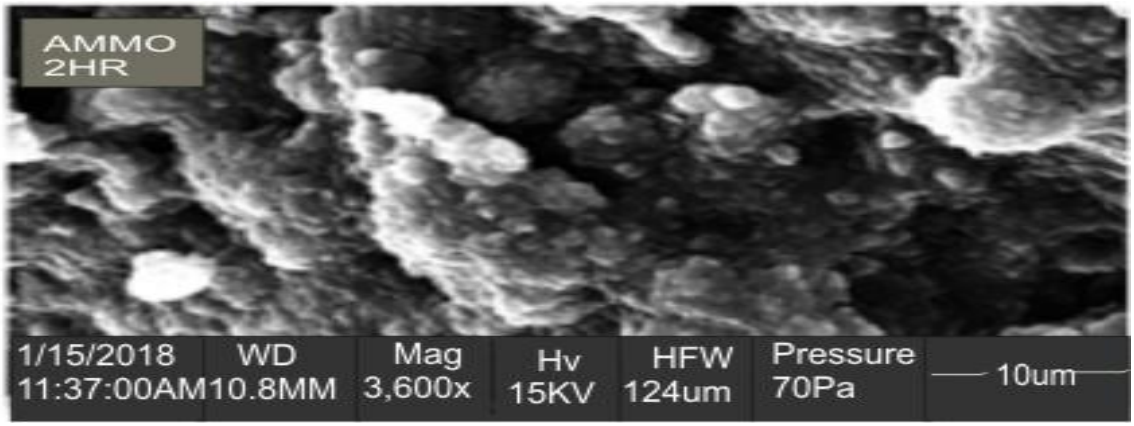

Figure 7: SEM Micrograph of the layer (0.1M) with Ammonia as complexing agent

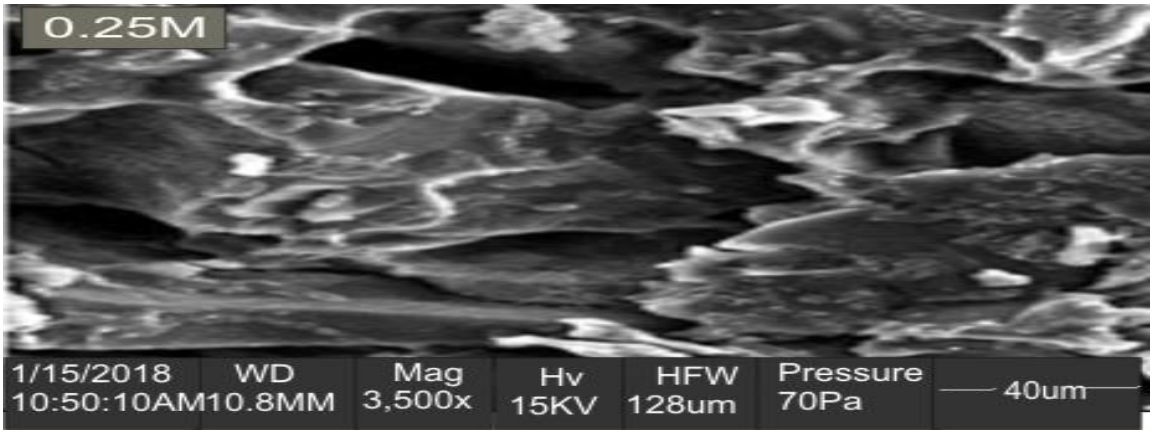

Figure 8: SEM Micrograph as-grown layer at 0.25 M

Figure 8 shows the SEM micrograph of the as-deposited film at a 0.25 M concentration. The analysis reveals a smoother surface with fewer irregularities compared to the 0.1 M film. Strong interactions between the NiO nanostructures at the interface are again evident, resulting in improved nanostructure morphology and greater uniformity, similar to the findings of Sureshm *et al*, (2014).

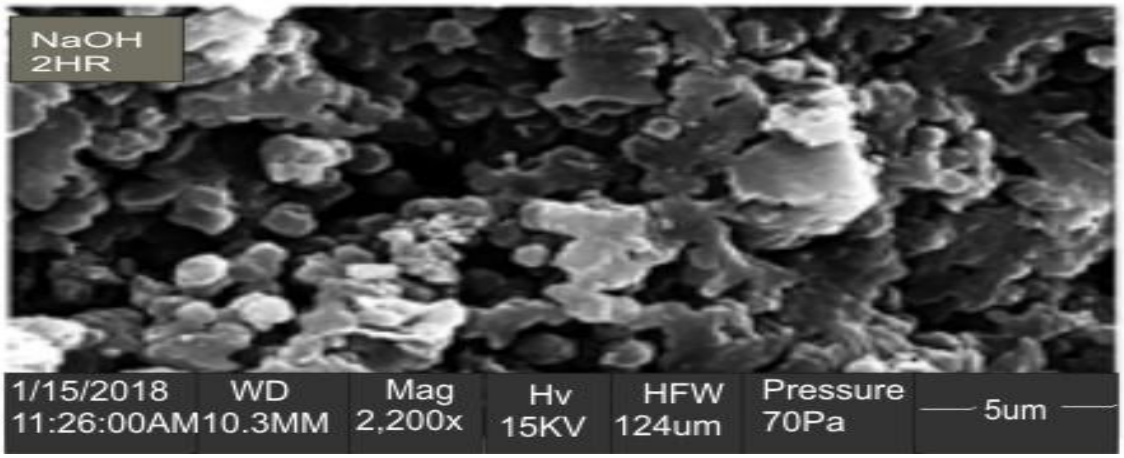

Figure 9: SEM Micrograph of the layer (0.25 M) with NaOH as complexing agent

Figure 9 presents the SEM micrograph of the 0.25 M film with NaOH as the complexing agent. The addition of NaOH enhanced the film's morphology, leading to a more uniform grain distribution. The CeO_2 doped with NiO film exhibited prominent grain boundaries, although the agglomeration was irregular in shape and size, as reported by Amita (2005).

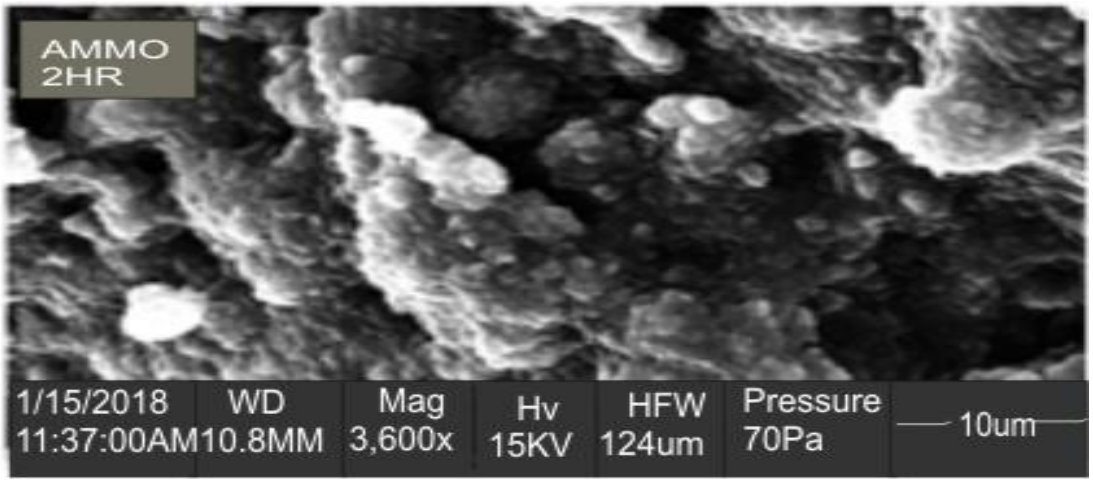

Figure 10: SEM Micrograph of the layer (0.25 M) with Ammonia as complexing agent

Figure 10 shows the SEM micrograph of the 0.25 M film with ammonia as the complexing agent. Similar to the 0.1 M ammonia-complexed film, the addition of ammonia improved the morphology, producing homogeneously shaped and sized grains that were tightly packed without visible pores. This film displayed better uniformity compared to the NaOH-complexed film, in agreement with the observations of Adele et al. (2003).

CONCLUSION

The impact of doping and the introduction of complexing agents on the optical and morphological properties of Thin films of nickel oxide (NiO) doped cerium oxide (CeO_2) using the chemical bath deposition (CBD) technique has been examined. The study revealed that sodium hydroxide, when used as a complexing agent, resulted in lower transmittance and band gap than ammonia at both 0.1 M and 0.25 M concentrations, suggesting that sodium hydroxide may have introduced more defects or impurities within the cerium oxide matrix. Interestingly, an increase in molar concentration was found to elevate the band gap energy. Additionally, the incorporation of nickel oxide as a dopant effectively increased the energy band gap of the cerium oxide films, enhancing their suitability for photovoltaic systems and UV protection. Morphological analysis demonstrated that complexing agents improved the uniformity and orientation of the films, leading to well-defined grain boundaries and reduced agglomeration. These characteristics suggest that nickel oxide (NiO) doped cerium oxide (CeO_2) holds significant potential for applications in solar energy, thermal control coatings, and UV radiation suppression.

ACKNOWLEDGMENT

The authors express their gratitude to those who provided the materials used in this research.

REFERENCES

Adele, Q. and Teresa, D. (2003). Anodic Electrodeposition of Cerium Oxide thin film. *Journal of the Electrochemical Society*, 158 (9), 248. https://iopscience.iop.org/article/10.1149/1.1596164/meta

Babitha, K. K., Sreedevi, A., Priyanka, K. P., Sabu, B., & Varghese, T. (2015). Structural characterization and optical studies of CeO2 nanoparticles synthesized by chemical precipitation. *Indian Journal of Pure & AppliedPhysics(IJPAP)*, *53*(9),596-603. http://op.niscpr.res.in/index.php/IJPAP/article/view/5542/0

Baisnab, D. K., Mukherjee, S., & Das, S. (2021). A short review on inorganic thin films from device perspective. *Chemical Solution Synthesis for Materials Design and Thin Film Device Applications*, 231-275. https://doi.org/10.1039/D1TA01291F

Bellardita, M., Fiorenza, R., Palmisano, L., & Scirè, S. (2020). Photocatalytic and photothermocatalytic applications of cerium oxide-based materials. In *Cerium Oxide (CeO_2): Synthesis, Properties and Applications* (pp. 109-167). Elsevier. https://doi.org/10.1016/B978-0-12-815661-2.00004-9

Channei, D., Nakaruk, A., Phanichphant, S., Koshy, P., & Sorrell, C. C. (2013). Cerium dioxide thin films using spin coating. *Journal of Chemistry*, *2013*(1), 579284. https://onlinelibrary.wiley.com/doi/abs/10.1155/2013/579284

Christian, N. I., Ekuma, A. P., Kingsley, O., & Ugah, J. O. (2023). Energy and Economic Evaluation of the 3000kwp Grid Connected Photovoltaic Power Plant in Umuoghara Quarry Industrial Cluster, Nigeria. *The*

Journals of the Nigerian Association of Mathematical Physics, *65*, 21-26. https://nampjournals.org.ng/index.php/home/article/view/4

Dalapati, G. K., Sharma, H., Guchhait, A., Chakrabarty, N., Bamola, P., Liu, Q., ... & Sharma, M. (2021). Tin oxide for optoelectronic, photovoltaic and energy storage devices: a review. *Journal of materials chemistry A*, *9*(31), 16621-16684. https://doi.org/10.1016/B978-0-12-819718-9.00007-8

Ershov, S., Druart, M. E., Poelman, M., Cossement, D., Snyders, R., & Olivier, M. G. (2013). Deposition of cerium oxide thin films by reactive magnetron sputtering for the development of corrosion protective coatings. *Corrosion science*, *75*, 158-168. https://doi.org/10.1016/j.corsci.2013.05.028

Göbel, M. C., Gregori, G., Guo, X., & Maier, J. (2010). Boundary effects on the electrical conductivity of pure and doped cerium oxide thin films. *Physical Chemistry Chemical Physics*, *12*(42), 14351-14361. https://pubs.rsc.org/en/content/articlelanding/2010/cp/c0cp00385a/unauth

Lavkova, J., Khalakhan, I., Chundak, M., Vorokhta, M., Potin, V., Matolin, V., & Matolinova, I. (2015). Growth and composition of nanostructured and nanoporous cerium oxide thin films on a foil. *Nanoscale*, *7*(9),4038-4047. https://pubs.rsc.org/en/content/articlelanding/2015/nr/c4nr06550f/unauth

Mary, J. A., Vijaya, J. J., Bououdina, M., & Kennedy, L. J. (2014). Simple microwave assisted solution combustion synthesis of cerium and nickel doped ZnO nanostructures: Effects on structural, morphological, optical, and magnetic properties. *Superlattices and Microstructures*, *76*, 174-185. https://doi.org/10.1016/j.spmi.2014.09.038

Melchionna, M., Trovarelli, A., & Fornasiero, P. (2020). Synthesis and properties of cerium oxide-based materials. In *Cerium Oxide (CeO_2): Synthesis, Properties and Applications* (pp. 13-43). Elsevier. https://doi.org/10.1016/B978-0-12-815661-2.00002-5

Nworie, I. C., Ele, U. S., Otah, P. B., Ojobeagu, A. O., Mbamara, C., Brown, N. W., & Ishiwu, S. M. U. (2024). Interdependence Of Deposition Time, Doping Concentration, and Annealing on the Optical Behavior of Mg-Doped Antimony Sulphide (Sb2S3) Thin Films. *The Journals of the Nigerian Association of Mathematical Physics*, *67*(2), 105-112. https://nampjournals.org.ng/index.php/home/article/view/386

Nworie, I. C., Ishiwu, S. M. U., Agbo, P. E., Ojobeagu, A. O., Otah, P. B., Mbamara, C., & Ojobo, B. (2024). Comparative Assessment of Optical and Solid-State Characteristics in Antimony-Doped Chalcogenide Thin Films of ZnSe and PbSe to Boost Photovoltaic Performance in Cells. *Nigerian Journal Physics*, *33*(1), 16-22. https://doi.org/10.62292/njp.v33i1.2024.202

Pankove, J. I. (1971). Optical Processes in Semiconductor, Prentic-Hall Inc., New Jersey, pp: 34-81.

Powalla, M., Paetel, S., Ahlswede, E., Wuerz, R., Wessendorf, C. D., & Magorian Friedlmeier, T. (2018). Thin-film solar cells exceeding 22% solar cell efficiency: An overview on CdTe-, Cu (In, Ga) Se2-, and perovskite-based materials. *Applied Physics Reviews*, *5*(4). https://pubs.aip.org/aip/apr/article/5/4/041602/998981

Sengupta, S., Aggarwal, R., & Golan, Y. (2021). The effect of complexing agents in chemical solution deposition of metal chalcogenide thin films. *Materials Chemistry Frontiers*, *5*(5), 2035-2050. https://pubs.rsc.org/en/content/articlelanding/2015/xx/d0qm00931h/unauth

Suresh, R., Ponnuswamy, V., & Mariappan, R. (2015). Effect of solvent and substrate temperature on morphology of cerium oxide thin films by simple nebuliser spray pyrolysis technique. *Materials Technology*, *30*(1),12-22. https://www.tandfonline.com/doi/abs/10.1179/1753555714Y.0000000183

Tsud, N., Skala, T., Mašek, K., Hanyš, P., Takahashi, M., Suga, H., Mori, T. and Yoshikawa, H. (2010). Cerium Oxide Stoichiometry Alteration via Sn Deposition: Influence of Temperature, *Journal of Electron Spectroscopy and Related Phenomena*, 169 (1), 20-25.